Chemical Geology 456 (2017) 98–111

Contents lists available at ScienceDirect

Chemical Geology

journal homepage: www.elsevier.com/locate/chemgeo

Chromium isotope systematics in the Connecticut River

Weihua Wu [a,b,*], Xiangli Wang [b], Christopher T. Reinhard [c], Noah J. Planavsky [b]

[a] Key Laboratory of Surficial Geochemistry, Ministry of Education, School of Earth Sciences and Engineering, Nanjing University, Nanjing 210093, China
[b] Department Geology and Geophysics, Yale University, CT 06511, USA
[c] School of Earth & Atmospheric Sciences, Georgia Institute of Technology, GA 30332, USA

ARTICLE INFO

Article history:
Received 18 August 2016
Received in revised form 27 February 2017
Accepted 4 March 2017
Available online 7 March 2017

Keywords:
Chromium isotopes
Redox proxy
The Connecticut River
Weathering
Climate

ABSTRACT

Limited constraints on Cr isotope fractionation during weathering and river transport is currently a gap in our understanding of the chromium (Cr) isotope system, which is an emerging proxy in environmental and paleoenvironmental studies. Here, we investigate Cr mobility and isotope fractionation from the temperate Connecticut River, USA, including Cr concentrations and isotopic compositions of river water, suspended particles, riverbed sediments, and weathering profiles. The δ^{53}Cr values of the Connecticut River water range from −0.17‰ to +0.92‰, which are similar to or higher than the weathered rocks in the catchment (−0.08‰ to −0.29‰). We find seasonal variations in dissolved δ^{53}Cr values in some but not all tributaries, suggesting that dissolved δ^{53}Cr is not a simple function of seasonality but may also be influenced by sub-catchment heterogeneity in lithology. In contrast to dissolved Cr, we found consistent seasonal difference in suspended Cr concentration and δ^{53}Cr. Suspended δ^{53}Cr is 0.1‰ higher than the unfractionated BSE in the fall (0.01–0.13‰), but indistinguishable from the BSE in the spring (−0.11‰ to 0.00‰). The suspended Cr concentration is also lower in the spring, and with higher Al-Mn-Fe concentrations. The lower suspended Cr concentration and δ^{53}Cr in spring may be linked to increased silicate and oxide load with depleted Cr due to stronger hydrological flux. Building from our dataset, there is not a consistent correlation with climate zones in a compilation of δ^{53}Cr and Cr concentration data from river water and weathering profiles, suggesting that climate is not a dominating factor controlling Cr isotopic behavior during weathering, suggesting that other factors (e.g., local catchment conditions and dissolved organic matter) may also be responsible for the observed river water δ^{53}Cr variability.

1. Introduction

There has been a recent increase in the extent of Cr isotope work, field in large part by the potential of Cr isotopes as paleoredox proxies. Chromium is a redox-sensitive transition metal (atomic number 24, group VI A) with two major valence states: hexavalent Cr(VI) and trivalent Cr(III). Cr (VI) exists as chromate (CrO_4^{2-}) and/or dichromate anions ($Cr_2O_7^{2-}$), which are highly soluble and a common carcinogenic pollutant in surface water and ground water systems. In contrast, Cr(III) is scarcely soluble at environmentally relevant pH, and easily absorbed onto solid surfaces (Elderfield, 1970; Bartlett and Kimble, 1976a, 1976b; Bartlett and James, 1979; Ross et al., 1981; James and Bartlett, 1983a, 1983b, 1983c; Rai et al., 1989; Manceau and Charlet, 1992; Fendorf, 1995; Kotaś and Stasicka, 2000).

Several factors contribute to redox transformations between Cr(III) and Cr(VI), including oxidation/reduction, precipitation/dissolution, and sorption/desorption reactions. It is accepted that manganese oxides are the primary environmental oxidant that converts insoluble Cr(III) to soluble Cr(VI) (e.g., Bartlett and James, 1979; Nakayama et al., 1981; Eary and Rai, 1987; Grohse et al., 1988; Fendorf and Zasoski, 1992; Fendorf, 1995), although an alternative oxidant, hydrogen peroxide (H_2O_2), may be locally important in areas with ultramafic rock (Oze et al., 2016). Conversely, soluble Cr(VI) can be reduced back to insoluble Cr(III) by a range of reductants such as soluble and solid-phase Fe(II) and S(-II), dissolved organic molecules, and microorganisms (Schroeder and Lee, 1975; Bodek et al., 1988; Eary and Rai, 1989; Rai et al., 1989; Fendorf, 1995; Fendorf and Li, 1996; Patterson et al., 1997; Pettine et al., 1998; Kim et al., 2001; Wielinga et al., 2001; Ellis et al., 2002; Sikora et al., 2008; Graham and Bouwer, 2009; Døssing et al., 2011; Han et al., 2012; Kitchen et al., 2012; Xu et al., 2015). Precipitation/dissolution reactions also play an important role, and are governed by the solubility of the chromium compound and the kinetics of dissolution (e.g., Sass and Rai, 1987; Bodek et al., 1988). Lastly, sorption/desorption reactions are relevant to the mobility of Cr (Freeze and

* Corresponding author at: Key Laboratory of Surficial Geochemistry, Ministry of Education, School of Earth Sciences and Engineering, Nanjing University, Nanjing 210093, China.
E-mail address: wuwh@nju.edu.cn (W. Wu).

http://dx.doi.org/10.1016/j.chemgeo.2017.03.009
0009-2541/

Cherry, 1979; Eary and Rai, 1989; Rai et al., 1989), for example, chromates can be adsorbed by amorphous aluminum, iron oxides, and organic complexes, and Cr(III) can be adsorbed onto silicacious components (James and Bartlett, 1983c; Bartlett and James, 1988).

Cr has four isotopes: ^{50}Cr (abundance 4.31%), ^{52}Cr (83.76%), ^{53}Cr (9.55%), and ^{54}Cr (2.38%). The variation of Cr isotopic compositions (δ^{53}Cr) in natural environment is primarily controlled by redox reactions (e.g. Ellis et al., 2002; Ellis et al., 2004; Schauble et al., 2004; Schoenberg et al., 2008). Cr isotopic fractionation during Cr(III) oxidation is poorly constrained, with values ranging from +1‰ to −2.5‰ (positive means the product is isotopically heavier than the reactant), depending on the oxidants (Bain and Bullen, 2005; Ellis et al., 2008; Wang et al., 2010; Zink et al., 2010). The variable fractionations are likely related to competition between kinetic and equilibrium isotope fractionation during oxidation (Zink et al., 2010; Wang et al., 2016b). During Cr transport to the ocean through river or groundwater systems, or within reducing marine environments, Cr(VI) can be partially reduced to Cr(III) with a preference for light isotopes, further enriching the Cr(VI) pool in higher δ^{53}Cr values if the reduction is incomplete (e.g., Ellis et al., 2002; Berna et al., 2010; Zink et al., 2010; Raddatz et al., 2011; Izbicki et al., 2012; Basu et al., 2014; Reinhard et al., 2014; D'Arcy et al., 2016; Gueguen et al., 2016).

The Cr isotopic system is unique, because in marked contrast to other redox tracers such as Mo or Fe, non-redox processes are thought to generate negligible Cr isotope fractionations (Ellis et al., 2004; Shauble et al., 2004). For over a decade, δ^{53}Cr has been used to monitor for reductive Cr(VI) remediation because of redox effects on Cr isotope fractionation (e.g., Ellis et al., 2002; Ball and Izbicki, 2004; Berna et al., 2010; Raddatz et al., 2011; Basu and Johnson, 2012; Izbicki et al., 2012; Jamieson-Hanes et al., 2012; Wanner et al., 2012). More recently, it has been used as a paleoredox proxy to reconstruct the evolution of Earth's ocean-atmosphere system (e.g., Frei et al., 2009; Crowe et al., 2013; Planavsky et al., 2014; Reinhard et al., 2014; Cole et al., 2016; Gilleaudeau et al., 2016; Holmden et al., 2016; Wang et al., 2016a; Wang et al., 2016c).

Applications of the Cr isotope system as a redox proxy requires a clear understanding of the global Cr cycle. While rivers are known to contribute a major source of Cr to oceans (e.g. Jeandel and Minster, 1987; Reinhard et al., 2013; McClain and Maher, 2016), δ^{53}Cr values of river waters, as well as Cr systematics under different climate regimes remain poorly constrained (e.g. Farkaš et al., 2013; Berger and Frei, 2014; Paulukat et al., 2015; D'Arcy et al., 2016). To move forward our understanding on this topic, we have examined Cr isotope fractionation at a catchment scale. Specifically, we present a record of Cr isotope data from river water, weathered catchment rocks, and bottom sediment from the temperate Connecticut River, providing preliminary constraints on the isotopic compositions of the suspended load as well as seasonal effects on the Cr system.

2. Regional setting

The Connecticut River is the largest and longest river in New England, and the third-largest river on the east coast of the United States (The Connecticut River Watershed Council, http://www.ctriver.org). The river originates near the U.S. border with Quebec, Canada, flows south for ~660 km, and empties into the Long Island Sound. It drains a total of 28,490 km^2 with an annual average discharge of 560 m^3/s, providing 70% of the Long Island Sound's freshwater (http://www.ctriver.org). The sediment yield of the Connecticut River is low (7.41×10^9 kg y^{-1}, Gordon, 1980), because much of its drainage basin was recently scoured by glaciation. For example, the upper and middle reaches of the Connecticut River are covered with glacial sediments and Paleozoic plutonic and metamorphic rocks (schists, amphibolites, gneisses, metavolcanics and metapelites). In the lower reaches, Mesozoic basalts are also exposed. Paleozoic Calcareous metasediments are also distributed along the river valley (Douglas et al., 2002; Reed et al., 2004) (Fig. 1).

3. Samples

We collected water and suspended particulate samples in October 2014 and April 2016. One river water sample was collected from the Mill River in November 2014 for testing analytical methods (Fig. 2, Table 1). We also sampled a few water samples from the Amazon River in Brazil in order to tentatively explore climate effects. For each sample, approximately two liters of water were collected about 3 m away from the riverbank and stored in acid-cleaned polyethylene bottles. Within 24 h after sampling, the pH values were measured and samples were filtered through acid cleaned 0.2 μm Whatman™ Nylon membranes. The filtered water samples were stored at 4 °C. Filter membranes were saved for suspended particulate analysis. During sampling we attempted to minimize anthropogenic influence by avoiding densely populated and industrial areas, as rivers flowing through industrial areas tend to have higher Cr concentrations (5–50 ng/mL, Wilber and Hunter, 1977; Vanderveen and Huizenga, 1981). There was no major rainfall a week prior to the sampling event.

The bottom sediment samples were collected roughly 3 m away from the river bank in October 2016. The sediments were centrifuged and the supernatant was discarded. A few grams of centrifuged sediments were then transferred into Teflon beakers and dried down at 60 °C on hot plates. The dry samples were powdered with an agate mill.

Several weathering profiles were sampled along the Connecticut River (Table 1) to provide a baseline for interpreting the results from the river water, sediments and suspended matter: a Triassic basalt profile along the tributary of the Westfield River (Fig. 3a, see GPS location in Table 1), a shale/siltstone profile along the tributary of the Farmington River (Fig. 3b), and a glacial till profile along the Deerfield River (Fig. 3c).

The ca. 10 m basalt overlies a metamorphosed shale unit (ca. 10 cm thick), and is cut through by a ca. 40 cm vertical fracture zone. Samples in this profile include an altered basalt within the fracture zone (SSP-1), two un-altered basalts adjacent to the altered zone (SSP-2 and SSP-5), two samples above (SSP-3) and below (SSP-4) the basalt-metashale contact, and one basalt floating in the top soil (SSP-6) that appears to be altered (Fig. 3a).

The Triassic shale/siltstone profile (Fig. 3b) is red, indicating sustained oxidative weathering. A total of five samples (WSP-1 to WSP-5, along strike in the exposed soil horizon) were taken from the same horizon to avoid syndepositional heterogeneities. The unit is more fractured on the left than on the right.

The glacial till profile was taken from a former gravel quarry (Fig. 3c). The profile can be divided into the following layers (from top to bottom): A ~15 cm dark topsoil rich in organic matter (GSP-0 and GSP-1), a ~25 cm brown horizon (GSP-2), a ~50 cm yellow silt layer (GSP-3), a ~35 cm gray silt/mud layer (GSP-4), a ~5 cm yellow silt layer (GSP-5), and finally a gray silt/mud layer with intercalated gravels (GSP-6). A total of seven samples (GSP-0 to GSP-6, from top to bottom) were collected from this profile.

4. Analytical methods

Solid rock samples were crushed in a ceramic jaw crusher and powdered with an agate mill. River sediments, glacial till, and shale samples were ashed at 500 °C for 8 h to remove organic matter before acid dissolution. About 0.1 g rock and sediment powders were dissolved in 2 mL concentrated HNO_3 and 2 mL HF on a hotplate. Samples were then dried and repeatedly flushed with 5 mL 6N HNO_3 and 5 mL 6N HCl to dissolve fluorides. Samples were finally dissolved in 4 mL 6N HCl for trace element and isotope analysis.

River water samples were evaporated and then redissolved in 4 mL 6N HCl. The suspended samples were treated with 10 mL aqua regia with 1 mL concentrated HF at 130 °C on a hotplate. The digested samples were evaporated to dryness and dissolved in 4 mL 6N HCl.

Trace element concentrations for all samples were measured on a Thermo Finnigan Element XR ICP-MS using multi-element

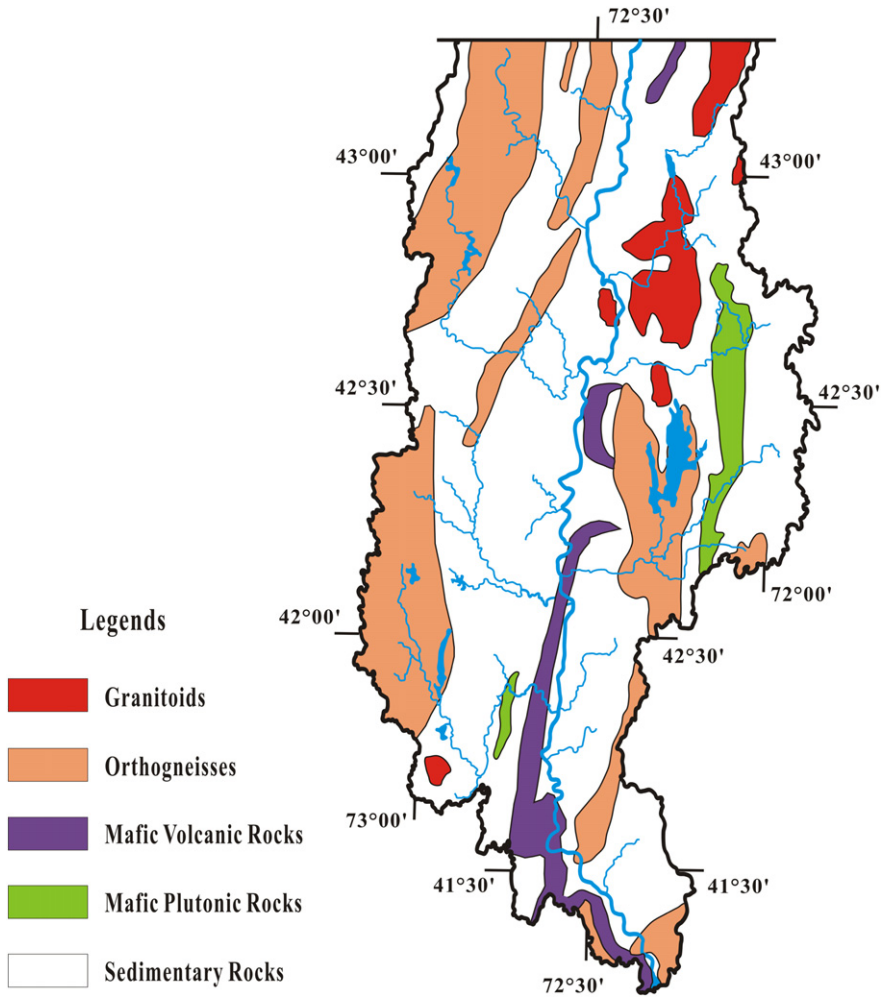

Fig. 1. Geological map of the Connecticut River.
(modified from Reed et al., 2004)

standard solutions with similar matrix elements to samples. Based on measured Cr concentrations, aliquots of acid digests containing 1 μg were spiked with appropriate amount of ^{50}Cr—^{54}Cr double spike before drying (Ellis et al., 2002; Schoenberg et al., 2008) to yield $(^{54}Cr)_{spike}/(^{52}Cr)_{sample}$ of ~0.5. The spike was added into the water samples and then evaporated to dryness. For river water, the dried samples were heated in aqua regia overnight at 100 °C on a hotplate (lids closed) to destroy organic matter. All samples bathed in 0.5 mL 6N HCl and left on a hotplate at ~100 °C until column procedures were performed.

For river sediments, suspended particles, and weathering profile samples with high Cr concentrations, Cr was purified following the anion exchange resin method (Schoenberg et al., 2008; Planavsky et al., 2014). For river water samples with low Cr concentrations, Cr was purified following the cation exchange method (Bonnand et al., 2011). For both methods, residual Fe was removed by a micro-column charged with 0.3 mL (inner diameter ~0.3 mm) anion exchange resin AG1-X8 (100–200 mesh). During the Fe microcolumn procedure, samples were dissolved in 0.2 mL 6N HCl, passed through the resin. Chromium was collected immediately after loading. An additional 0.4 mL 6N HCl was used to completely elute any remaining Cr.

Chromium isotopic compositions were measured on a Neptune Plus MC-ICP-MS housed at the Yale Metal Geochemistry Center. Purified Cr samples were dissolved in ~0.7 N HNO_3 with concentrations of ~250 ng/g and 50 ng/g for sediments/suspended particles and water samples, respectively, and introduced to the plasma with a PFA μFlow nebulizer (~50 μL/min) coupled with an Apex IR desolvation introduction system (Elemental Scientific) without additional gas or membrane desolvation. With a standard sample cone and X skimmer cone and under high-resolution mode, the obtained sensitivity was 15–75 pA ^{52}Cr per 1 μg/g Cr. All ion beams were measured on Faraday detectors connected to $10^{11}\Omega$ amplifiers. The isotopes ^{49}Ti, ^{51}V, and ^{56}Fe were measured to monitor and correct for isobaric interferences of ^{50}Ti, ^{50}V, and ^{54}Fe. The unprocessed NIST SRM 979 standard was analyzed after every three samples to monitor potential drift, which was <0.1‰ within each analytical session. On-peak blanks were measured before and after every sample/standard and subtracted before the double spike data reduction (cf. Johnson et al., 1999).

The total procedural Cr blank was <0.6 ng for water samples, and ~2 ng for sediments, weathering profiles and suspended particles. These blanks were very small relative to the amount of Cr in the samples (<1%). The analytical accuracy and precision for water samples and sediments/suspended particles were assessed by repeatedly processing and measuring USGS reference materials BHVO-2 and NIST SRM 3112 standard . Measured SRM 3112a (-0.07 ± 0.06‰, 2SD, n = 7) and BHVO-2 (-0.09 ± 0.03‰, 2SD, n = 8) (Table 2) are consistent with previous measurements (e.g. Schoenberg et al., 2008; Wang et al., 2016b, 2016c).

5. Results

Sample information and pH data are given in Table 1 (no pH values were acquired in April 2016), and Cr isotope and concentration data are presented in Table 3. The pH values of October 2014 river water samples

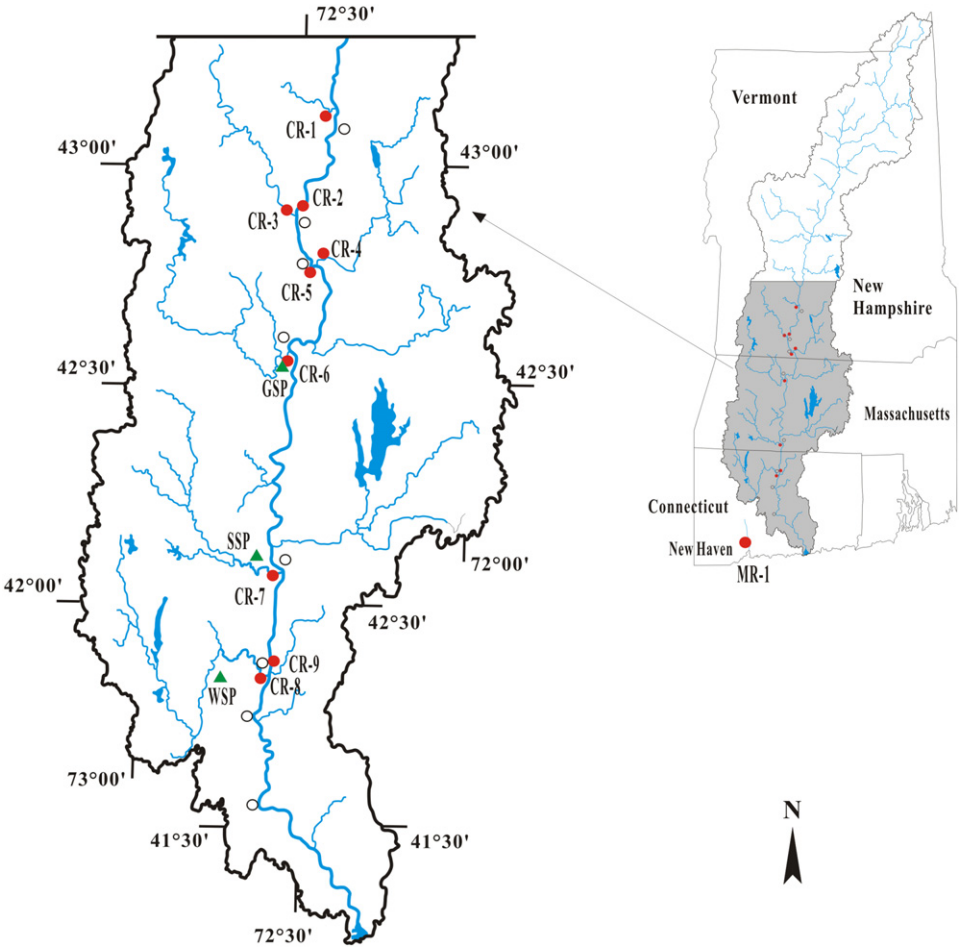

Fig. 2. A map of the Connecticut River basin (modified from the Connecticut River Watershed Council, http://www.ctriver.org). The red circles are sampling locations for rivers water and sediments, and the green triangles are for weathering profiles. The cities (open circles) from upstream to downstream are: Walpole, Brattleboro, Hinsdale, Greenfield, Springfield, Windsor, Harford, and Middletown. MR–1 is for the Mill River (a small river about 50 km west of the Connecticut River).

range from 7.04 to 7.58 (Table 1). The δ^{53}Cr values of the Connecticut River range from −0.17‰ to 0.90‰, similar to other studied rivers (Frei et al., 2014; Paulukat et al., 2015; D'Arcy et al., 2016), but lower than some rivers draining serpentinite rocks (up to 4‰, Farkaš et al., 2013; Novak et al., 2014). No correlation between pH and Cr concentration or δ^{53}Cr values is found (see Rai et al., 1987 for a relationship between Cr solubility and pH). The dissolved Cr concentration in Connecticut River water (1.7–6.2 nM, or 0.1–0.3 ng/mL) is lower than other rivers worldwide (2–1730 nM, or 0.1–86.5 ng/mL, Dojlido and Best, 1993), and is also below the discharge-weighted global average riverine input value of ~15 nM or ~0.75 ng/mL (Reinhard et al., 2013). There is no clear correlation between Cr concentration and δ^{53}Cr values, both in October 2014 and April 2016 (Fig. 4A).

There was a clear difference in the δ^{53}Cr and Cr concentrations in suspended particles between or two (spring and fall) sampling times. The δ^{53}Cr values of October 2014 suspended samples range from 0.01‰ to 0.13‰, which are ~0.1‰ higher than April 2016 samples that range from −0.01‰ to −0.11‰ (Fig. 4B, Table 3). October samples are slightly fractionated from the BSE while April samples are indistinguishable from BSE (Fig. 4B, Table 3). The Cr concentration of April 2016 suspended samples (1.25 to 6.33 ng/mL) are generally higher than October 2014 samples (0.57 to 0.94 ng/mL) (Fig. 4B; Table 3). In

Table 1
Sample information.

Num.	River Basins	Cities	Date	Latitude	Longitude	Elevation (m)	pH
CR-1	West River	Walpole	10/29/15	42°52′37.49″	72°34′19.89″	67	7.37
CR-2	Connecticut River	Brattleboro	10/29/15	42°52′16.55″	72°33′19.10″	68	7.56
CR-3	Saxtons River	Brattleboro	10/29/15	43°07′24.24″	72°26′29.31″	75	7.58
CR-4	Ashuelot River	Hinsdale	10/29/15	42°47′08.76″	72°29′08.99″	65	7.10
CR-5	Connecticut River	Hinsdale	10/29/15	42°46′01.81″	72°30′05.38″	66	7.45
CR-6	Deerfield River	Greenfield	10/29/15	42°34′11.52″	72°35′13.23″	35	7.24
GSP-(0–6)	Deerfield River	Greenfield	6/14/15	42°33′17.0″	72°33′49.7″		
CR-7	Westfield River	Springfield	10/29/15	42°05′2.10″	72°35′39.90″	12	7.32
SSP-(1–6)	Westfield River	Springfield	6/14/15	42°06′22.9″	72°40′52.0″		
CR-8	Farmington River	Windsor	10/29/15	41°50′44.41″	72°38′22.60″	10	7.04
WSP-(1–5)	Farmington River	Windsor	6/14/15	41°53′19.0″	72°46′29.2″		
CR-9	Connecticut River	Windsor	10/29/15	41°50′52.30″	72°37′25.15″	6	7.33
MR-1	Mill River	New Haven	11/23/15	41°19′33.60″	72°54′32.10″	14	

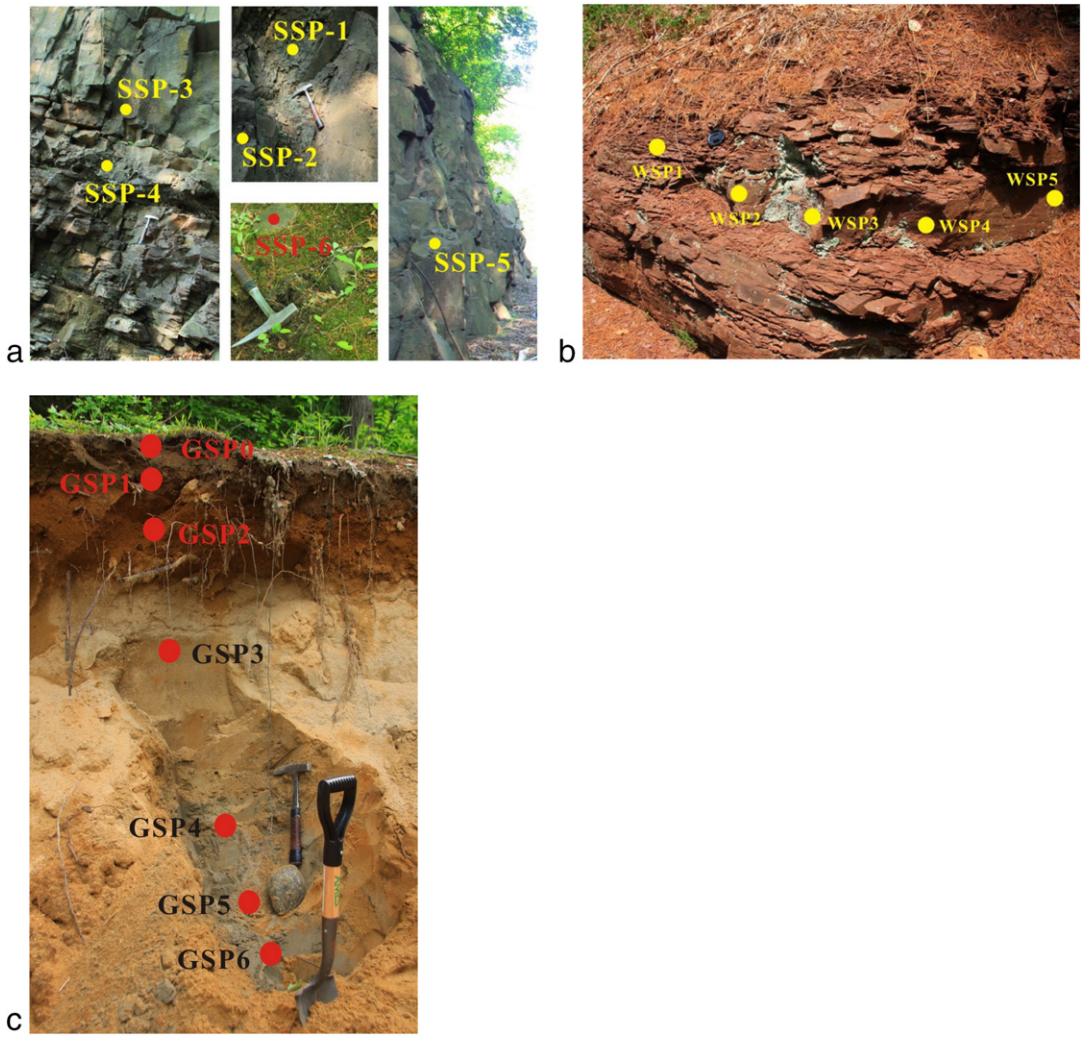

Fig. 3. Three weathering profiles: (a) The basalt weathering profile along the tributary Westfield River; (b) The shale/siltstone weathering profile exposed by a road cut along the tributary Farmington River; (c) A glacial till profile exposed in a quarry along the tributary Deerfield River.

order to examine Cr depletion/enrichment and its migration in weathering profiles and catchments, Cr concentrations are normalized to Al concentrations because Al is considered immobile during weathering (Frei et al., 2014; Babechuk et al., 2016; Holmden et al., 2016). After normalization, the Cr/Al ratios of April 2016 samples (0.0007 to 0.0183) are generally lower than October 2014 samples (0.0018 to 0.0356) ($p = 0.017$, Mann-Whitney statistic = 68) (Fig. 4D; Table 4).

Fe and Mn concentrations in suspended particles are plotted in Fig. 4E–H. Suspended Fe concentrations in April are statistically higher than those in October ($p = 0.006$, Mann-Whitney U rank test, Table 4), but Mn concentrations show no statistically significant difference ($p = 0.058$; Table 4; Fig. 4F). The ratio of Mn/Fe generally follow the expected trend (Fig. 4E) predicted by the upper continental crust, or UCC (Rudnick and Gao, 2003). Higher Fe-Mn suspended samples contain lower Cr/Al ratios (Fig. 4G–H; Table 4).

There is no obvious climatic effect on dissolved Cr (Fig. 4A), except when each tributary is evaluated individually (Fig. 5). Some, but not all tributaries show differences in δ^{53}Cr between the two sampling sessions (Fig. 5A). For example, samples CR-3, CR-4, CR-5, CR-7, and CR-8 have similar δ^{53}Cr values between two sampling sessions, while samples CR-1 and CR-9 show large seasonal differences. For Cr concentrations, all samples show discernable differences between October and April. Five out of seven samples (with available data) show higher Cr concentration in October (0.09–0.32 ng/L) than in April (0.06–0.11 ng/mL).

Bottom sediments were measured only in October 2014 and their δ^{53}Cr values (−0.02‰ to −0.16‰, Table 2) are indistinguishable from the BSE (Fig. 6). The sediment Cr concentrations (20 to 138 μg/g, averaged 58.7 μg/g) are close to those in some large rivers, such as

Table 2
Standard values (processed through the same procedures as samples).

	ng Cr used	δ^{53}Cr	2se
SRM3112a	50	−0.02	0.07
	100	−0.07	0.04
	50	−0.05	0.06
	100	−0.06	0.04
	100	−0.08	0.01
	100	−0.08	0.02
	100	−0.13	0.01
BHVO-2	100	−0.08	0.04
	100	−0.08	0.04
	100	−0.09	0.04
	100	−0.10	0.04
	100	−0.09	0.04
	100	−0.08	0.04
	100	−0.12	0.04

Table 3
Element and Cr isotope data for water, suspended particulate, sediments, and weathering profile samples. Note that Cr concentration units for rock samples are μg/g, but for water and suspended samples are ng/ml.

	Samples	δ^{53}Cr	2σ	Cr	Al	Fe	Mn
Shale/siltstone profile (altered)	WSP-1	−0.08	0.05	114.67	102,674.68	72,003.80	611.13
Shale/siltstone profile (altered)	WSP-2	−0.20	0.05	49.61	52,017.16	29,236.19	615.10
Shale/siltstone profile (altered)	WSP-3	−0.15	0.05	37.47	50,419.32	23,203.11	420.17
Shale/siltstone profile (altered)	WSP-4	−0.21	0.04	42.27	48,264.55	24,829.77	381.31
Shale/siltstone profile (altered)	WSP-5	−0.19	0.04	56.31	55,355.53	29,182.41	470.88
Glacial till profile (soil)	GSP-0	−0.18	0.04	39.81	49,503.15	33,766.53	841.19
Glacial till profile (soil)	GSP-1	−0.12	0.05	33.13	45,870.26	32,336.75	895.34
Glacial till profile (silt)	GSP-2	−0.12	0.04	35.28	50,023.12	33,651.11	813.98
Glacial till profile (silt)	GSP-3	−0.22	0.04	29.22	45,721.29	29,017.54	856.33
Glacial till profile (silt/mud)	GSP-4	−0.29	0.04	61.88	71,419.27	46,476.87	1018.98
Glacial till profile (silt)	GSP-5	−0.20	0.04	50.42	61,395.89	66,998.32	2007.26
Glacial till profile (silt/mud)	GSP-6	−0.23	0.04	67.63	85,604.09	45,813.46	894.34
Basalt profile (altered)	SSP-1	−0.20	0.05	65.31	57,063.74	109,758.52	1494.29
Basalt profile (un-altered)	SSP-2	−0.26	0.04	72.47	60,243.84	133,641.16	1726.63
Basalt profile (un-altered)	SSP-3	−0.15	0.04	59.57	57,291.61	70,408.01	951.15
Basalt profile (altered)	SSP-4	−0.16	0.03	76.49	60,492.39	60,768.34	559.84
Basalt profile (un-altered)	SSP-5	−0.27	0.03	70.98	52,590.82	131,793.52	1947.08
Basalt profile (altered)	SSP-6	−0.17	0.04	42.29	52,497.16	42,727.35	1209.36
Bottom sediments	CR-1	−0.13	0.04	129.75	60,690.03	47,634.46	1061.91
Bottom sediments	CR-2	−0.14	0.04	52.80	51,432.45	32,733.18	771.24
Bottom sediments	CR-4	−0.10	0.04	23.18	44,760.91	16,388.79	1044.94
Bottom sediments	CR-5	−0.14	0.04	53.82	48,639.57	32,620.82	1111.10
Bottom sediments	CR-6	−0.13	0.04	59.92	52,402.46	59,013.73	2243.79
Bottom sediments	CR-7	−0.03	0.04	72.24	61,450.17	41,285.75	860.32
Bottom sediments	CR-8	−0.08	0.04	49.20	57,861.81	32,938.31	1007.25
Bottom sediments	CR-9	−0.08	0.04	28.40	40,598.71	16,522.40	316.89
River Water - October 2014	CR-1	−0.17	0.07	0.32			
River Water - October 2014	CR-2						
River Water - October 2014	CR-3	0.82	0.06	0.11			
River Water - October 2014	CR-4	0.16	0.06	0.10			
River Water - October 2014	CR-5	0.53	0.06	0.09			
River Water - October 2014	CR-6						
River Water - October 2014	CR-7	0.83	0.06	0.09			
River Water - October 2014	CR-8	0.90	0.06	0.15			
River Water - October 2014	CR-9	0.79	0.06	0.12			
Mill River Water - October 2014	MR-1	1.02	0.05	0.52			
River Water - April 2016	CR-1	0.40	0.04	0.11	42.35	28.80	6.77
River Water - April 2016	CR-2	0.37	0.04	0.13	34.67	32.93	23.20
River Water - April 2016	CR-3	0.78	0.04	0.12	29.79	19.67	3.75
River Water - April 2016	CR-4	0.32	0.04	0.06	27.42	32.84	4.88
River Water - April 2016	CR-5	0.37	0.04	0.12	26.53	25.13	5.91
River Water - April 2016	CR-6	0.36	0.04	0.11	49.97	40.27	4.34
River Water - April 2016	CR-7	0.75	0.04	0.06	18.90	22.99	2.27
River Water - April 2016	CR-8	0.92	0.04	0.09	11.47	23.64	1.65
River Water - April 2016	CR-9	0.26	0.04	0.09	29.39	44.71	2.11
Suspended - October 2014	CR-1	0.01	0.03	1.06	34.38	98.97	1.31
Suspended - October 2014	CR-2	0.01	0.02	0.64	23.73	103.96	3.63
Suspended - October 2014	CR-3	0.13	0.02	1.03	28.91	97.12	1.58
Suspended - October 2014	CR-4	0.06	0.02	1.19	62.22	156.68	5.01
Suspended - October 2014	CR-5	0.09	0.02	0.68	102.59	115.44	5.49
Suspended - October 2014	CR-6	0.07	0.02	1.02	564.69	251.03	10.31
Suspended - October 2014	CR-7	0.07	0.02	0.75	50.73	80.98	7.50
Suspended - October 2014	CR-8	0.07	0.02	0.87	54.03	98.64	7.34
Suspended - October 2014	CR-9	0.08	0.02	0.81	115.65	176.57	10.97
Suspended - April 2016	CR-1			1.25	109.14	112.92	1.65
Suspended - April 2016	CR-2	−0.11	0.03	1.84	987.02	510.68	19.36
Suspended - April 2016	CR-3	−0.09	0.04	1.37	201.44	163.55	3.00
Suspended - April 2016	CR-4	−0.02	0.04	1.20	191.76	265.20	8.09
Suspended - April 2016	CR-5	−0.03	0.03	1.76	1018.38	502.16	16.65
Suspended - April 2016	CR-6	−0.10	0.01	1.45	260.12	200.21	7.50
Suspended - April 2016	CR-7	0.00	0.04	1.99	1316.19	546.77	30.30
Suspended - April 2016	CR-8	−0.01	0.03	1.63	89.07	169.09	17.96
Suspended - April 2016	CR-9	−0.07	0.03	6.33	9638.21	4356.67	90.64

Brahmaputra, Yangtze, Yellow River (Du et al., 2011 and references therein), but lower than the rivers in the Deccan basalt province (100–306 μg/g, Das and Krishnaswami, 2007). The Cr/Al ratios in bottom sediments are generally lower than the BSE (except for sample CR-1, Fig. 5F).

The δ^{53}Cr values for the investigated basalt samples (both visually altered and unaltered) range from −0.15‰ to −0.27‰, which are at the lower end of, or slightly negatively fractionated from the BSE (−0.1 ± 0.1‰, Schoenberg et al., 2008). The Cr/Al ratios (0.0010–0.0013) do not differ between altered (SSP-1, 3, 4, 6) and unaltered (SSP-2, 5) basalts, which are similar to the UCC (0.0011, Rudnick and Gao, 2003).

The δ^{53}Cr values for the weathered shale/siltstone samples are also at the lower end of the BSE values (Table 3; Fig. 6). The severely weathered portion on the left (WSP-1) appear to have higher δ^{53}Cr values (−0.08‰) than those of the relatively less weathered portion (−0.19‰), although the total variation (0.11‰ difference) is within

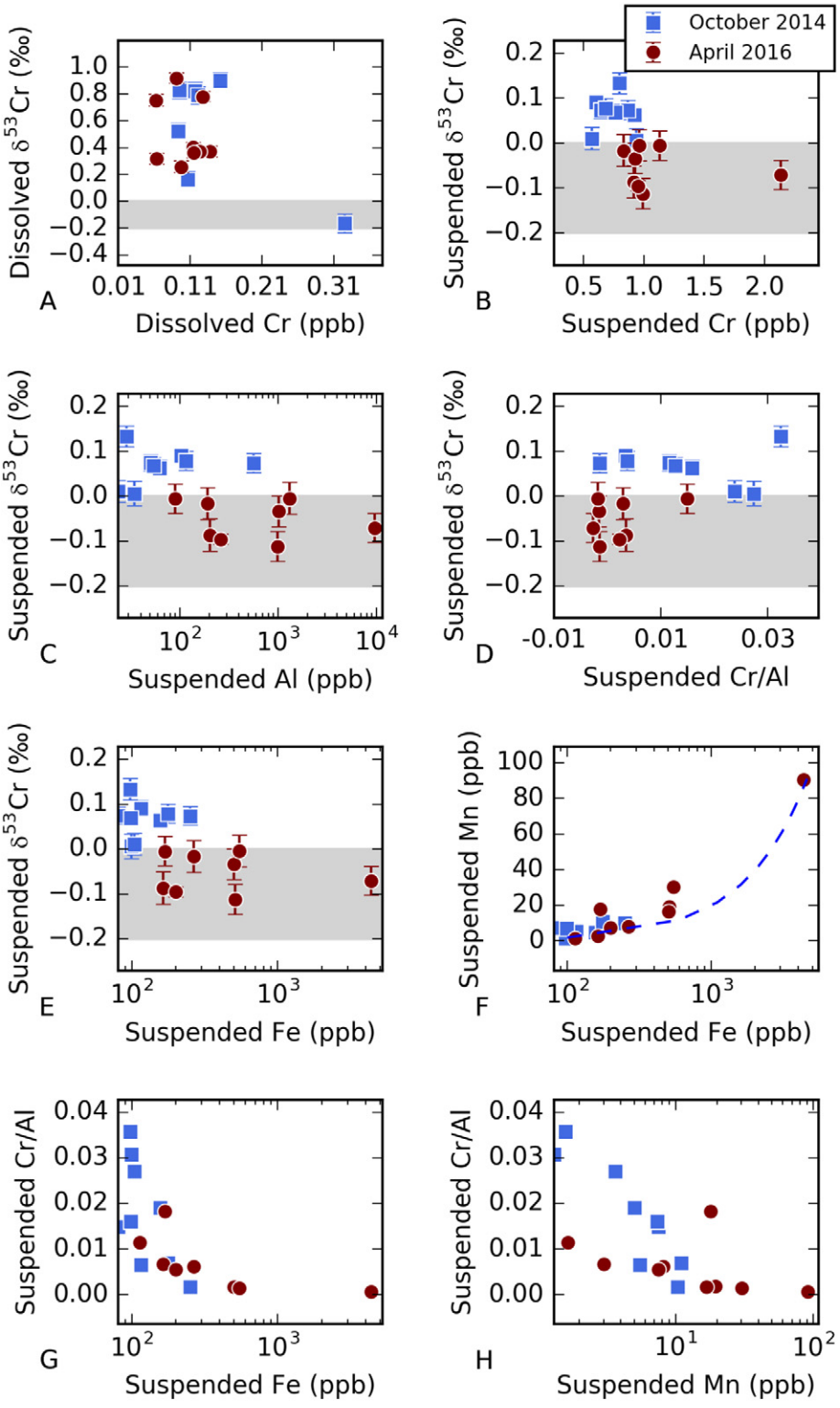

Fig. 4. Correlation between δ^{53}Cr, Cr, Al, Fe, and Mn concentrations. All figures share the same legend as B. The gray bars in A–E represent the unfractionated BSE (Schoenberg et al., 2008). The dashed curve in F represents the expected relationship between Mn and Fe concentration in average upper continental crust (Rudnick and Gao, 2003). Notice the log scale of the x-axes in C,E, F, G, and H.

the analytical error. The Cr/Al ratios in this profile (0.0007–0.0011) are similar to, or slightly lower than the average value for the UCC.

The δ^{53}Cr values in the glacial till profile are again at the lower end of, or slightly lower than the BSE (Table 3; Fig. 6). Samples in the lower section (−0.23‰) have slightly more negative δ^{53}Cr values than those in the upper section (−0.12‰), but again the difference is within the analytical error. All samples in this profile have Cr/Al ratios (0.0006–0.0009) much lower than the UCC (0.0011).

Table 4
Unparameterized Mann-Whitney U rank tests.

	April 2016 compare to October 2014	p value
Dissolved δ^{53}Cr	Same	0.185
Dissolved Cr	Same	0.130
Suspended δ^{53}Cr	Lower	0.006
Suspended Cr	Higher	0.003
Suspended Al	Higher	0.004
Suspended Cr/Al	Lower	0.017
Suspended Fe	Higher	0.006
Suspended Mn	Same	0.058

6. Discussion

6.1. Dissolved Cr

The δ^{53}Cr values of global seawater follow a Rayleigh type fractionation model, which is suggested as a result of partial reduction of Cr(VI) in surface waters (Scheiderich et al., 2015). Lack of this correlation in the Connecticut River and other global rivers (compiled in Fig. 7A) suggests that Cr concentration and δ^{53}Cr in rivers are also controlled by other processes, such as the weatherability, Cr content, and δ^{53}Cr of the local catchment lithology in individual tributaries. Interestingly, although serpentinite catchment lithology (e.g., India and the Czech Republic) generates higher dissolved Cr concentration in rivers compared to other catchment lithologies such as basalt, their δ^{53}Cr values are similar (this study; Berger and Frei, 2014; Frei et al., 2014; Novak et al., 2014; Paulukat et al., 2015; D'Arcy et al., 2016).

6.2. Suspended Cr

Suspended Cr could have several Cr species, including adsorbed Cr(VI), adsorbed ligand-bound Cr(III), colloidal Cr(III), clay-bound Cr(III). Adsorbed Cr(VI) should inherit high δ^{53}Cr values from dissolved Cr(VI); ligand-bound Cr(III) δ^{53}Cr values are currently unconstrained due to lack of experimental data; colloidal Cr(III) δ^{53}Cr values results from hydrolysis of Cr(III) sourced from Cr(VI) reduction, or from ligand-bound Cr(III); clay-bound Cr(III) δ^{53}Cr values are expected to be unfractionated from the BSE values (e.g., Gueguen et al., 2016). The δ^{53}Cr of Cr(III) sourced from Cr(VI) reduction can vary widely depending on the δ^{53}Cr of Cr(VI) and the extent of reduction. Further, the proportion each Cr pool listed above ultimately determines the δ^{53}Cr of the suspended particles.

The δ^{53}Cr values of suspended samples in April 2016 are within the BSE range, suggesting dominance of unfractionated, potentially detrital Cr. Normalizing Cr to Al concentrations changed the direction of the Cr concentration trend between our two sampling sessions (April and October (Fig. 4B–D)), confirming that higher Cr concentrations found in April samples are indeed because of increased suspended silicate component represented by high Al concentration.

Fe and Mn are closely linked with Cr cycling because of adsorption of Cr to iron oxides and oxidation of Cr(III) by Mn oxides (Ellis et al., 2002; Ellis et al., 2004; Wang et al., 2010; Nakayama et al., 1981). Higher Fe (and potentially higher Mn) in April samples suggest higher oxide load. However, higher oxides did not have a significant influence on the δ^{53}Cr of suspended Cr, as adsorption would inherit dissolved Cr(VI) δ^{53}Cr and thus should have made the suspended Cr isotopically heavy. Instead, the inverse correlation between Cr/Al and Fe and Mn (Fig. 4G–H) suggests that April 2016 samples have higher oxide and silicate components that are relatively depleted in Cr concentration. One possible explanation for the depleted Cr concentration in suspended particles could be oxidation of Cr(III) by manganese oxides, which is also consistent with the fact that oxidation generally releases isotopically heavy Cr and thus leads to isotopically light Cr in the residual, consistent with the observed low δ^{53}Cr in suspended particles.

6.3. Cr speciation

Thermodynamic equilibrium predicts that Cr(VI) should be the predominant dissolved Cr species in seawater (Elderfield, 1970). However, a significant amount of Cr(III) (~10% to ~100%) is found in river, estuary, and open ocean waters (Elderfield, 1970; Comber and Gardner, 2003)—much higher than thermodynamic predictions. Because of the very low solubility of Cr(III) (Rai et al., 1987), such high dissolved Cr(III) concentration at pH 7–8 suggests that Cr(III) is stabilized in solution by some chemical component, likely dissolved organic matter (e.g. Nakayama et al., 1981; James and Bartlett, 1983a, 1983b, 1983c). Dissolved Cr(III) could be sourced from ligand mobilization of insoluble Cr(III) contained in catchment rocks, or from reduction of dissolved Cr(VI). Currently, experimental Cr isotope fractionation during organic ligand mobilization is lacking, but fractionation is expected to be small given that non-redox reactions generally induce small isotope fractionations in the Cr system (Ellis et al., 2002; Ellis et al., 2004; Schauble et al., 2004; Schoenberg et al., 2008; Wang et al., 2015). Indeed, experiments show that Cr(VI) reduction produces Cr(III) with relatively low δ^{53}Cr values offset from the remaining Cr(VI) by a constant value (Ellis et al., 2002; Døssing et al., 2011; Kitchen et al., 2012; Basu et al., 2014). However, given Cr(VI) is isotopically heavy (Ellis et al., 2002; Ellis et al., 2004; Schauble et al., 2004; Schoenberg et al., 2008; Wang et al., 2015 due to oxidation), reduction of Cr(VI) could produce Cr(III) with either positive or negative δ^{53}Cr, depending on the isotope fractionation factor and extent of reduction. In sum, the measured dissolved δ^{53}Cr values in this study are likely mixed values of dissolved Cr(III) and Cr(VI). Future work on δ^{53}Cr values of dissolved Cr(III) is needed to investigate the true values of dissolved Cr(VI) produced by oxidative weathering.

6.4. Anthropogenic influences

The Cr concentrations in all of our water samples are very low (0.088 to 0.938 ng/mL and 0.056 to 0.133 ng/mL for the samples in October 2014 and April 2016, respectively). These values are comparable to rainwater samples collected in Lenox Mountain, MA and Wilmington, NC, USA with dissolved Cr concentrations from 2.4 to 2.7 nM, or 0.12 to 0.14 ng/mL (Kieber et al., 2002 and references therein). In comparison, rivers flowing through industrial areas have much higher Cr concentrations, ranging from 5 to 50 ng/mL (Wilber and Hunter, 1977; Vanderveen and Huizenga, 1981). In sum, it is unlikely that our Connecticut River water samples are influenced by anthropogenic sources. In comparison, the sample of the Mill River (MR-1), which is near a former industrial city (New Haven, CT), has a more positive δ^{53}Cr value (+1.02‰) and high Cr concentration (0.52 ng/g), and was likely influenced by anthropogenic activities.

6.5. Spatiotemporal variation of δ^{53}Cr and Cr concentration

We sampled over two sessions, and the differences in δ^{53}Cr values between these two sessions in some tributaries suggestes a seasonal evolution in the riverine δ^{53}Cr flux. Foremost, a strong difference in δ^{53}Cr between October 2014 and April 2016 samples is found in some tributaries in the Connecticut River system (CR-1 and CR-9). CR-1 has a much lower δ^{53}Cr value in October relative to April, while CR-9 shows the opposite trend (Table 3; Fig. 5). Although additional work is needed, this inverse direction of change at these two sites suggests that seasonality (precipitation and temperature) is not the major control of the dissolved δ^{53}Cr. Samples CR-3, CR-7, and CR-8 show similar δ^{53}Cr values between two sampling events, and the δ^{53}Cr values in these three samples are much higher than other samples in both seasons. This suggests that in these tributary catchments, factors such as lithology (likely types of rocks uncharacterized in this study) play a more important role than seasonality (temperature and precipitation) in

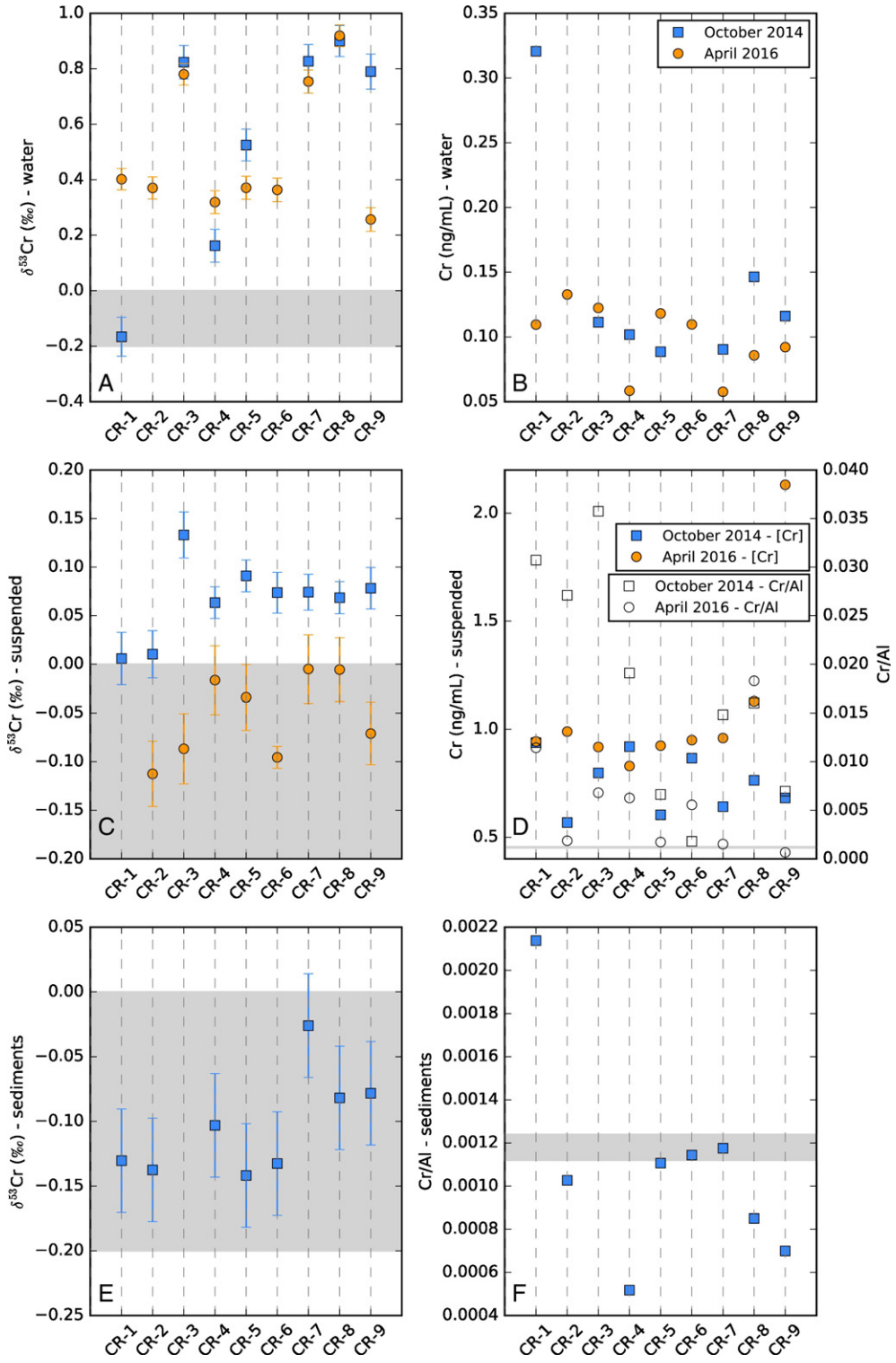

Fig. 5. Seasonality effects on Cr isotope systematics in the Connecticut River system. A & B: dissolved Cr; C and D: suspended Cr; E & F: bottom sediment Cr. Horizontal gray bars are the δ^{53}Cr and Cr/Al ranges of the bulk silicate earth and average upper continental crust, respectively ($\delta^{53}Cr_{BSE} = -0.1 \pm 0.1‰$, Schoenberg et al., 2008; $Cr/Al_{UCC} = 0.0011 \pm 10\%$, Rudnick and Gao, 2003).

controlling river δ^{53}Cr values. This catchment-specific variability is consistent with previous river Mo isotope studies that found high Mo isotope variability among catchments with different sizes and bed rock lithology (e.g., Neubert et al., 2011).

Interestingly, the δ^{53}Cr value of West River tributary (CR-1) in October value falls within the unfractionated BSE range (−0.17‰), in sharp contrast to its April value (+0.4‰) (Fig. 5A). This sample also has the highest observed Cr content in water, sediment, and suspended particulates in October (Fig. 5B), suggesting that the dissolved Cr in this water sample may be dominated by unfractionated Cr, likely Cr(III) complexed with organic molecules. Several studies show that Cr(III) complexes form when Cr(VI) is reduced by soil organic material, and the resulting complexes may be very stable (James and Bartlett, 1983a, 1983b; Fendorf, 1995; Kimbrough et al., 1999).

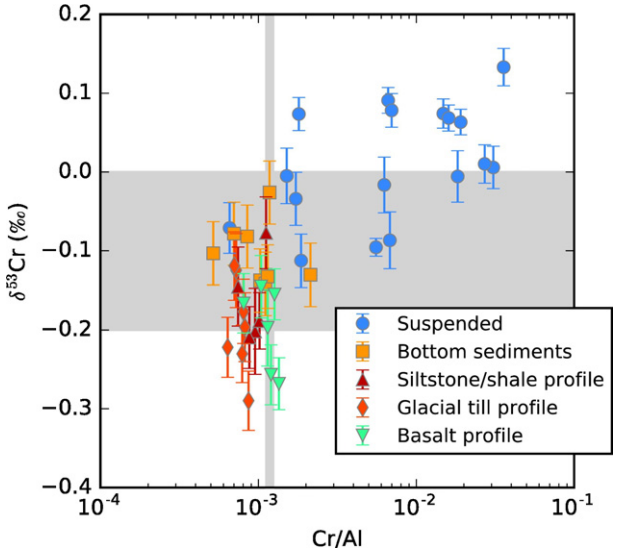

Fig. 6. Cross plot of δ^{53}Cr vs. Cr/Al in suspended and rock/sediment samples in the Connecticut River system. The suspended particle samples include October 2014 and April 2016 samples. Horizontal and vertical bars represent the δ^{53}Cr and Cr/Al ranges of the BSE and average upper continental crust, respectively ($\delta^{53}Cr = -0.1 \pm 0.1$‰, Cr/Al = 0.0011 ± 10%. Schoenberg et al., 2008; Rudnick and Gao, 2003).

In contrast to river waters, suspended particles show a consistent difference between spring and fall seasons. For example, δ^{53}Cr values of suspended samples in April 2016 are ~0.1‰ lower, with concentrations 1.0–7.8 times higher than samples collected in October 2014 (Fig. 5C–D). Further, Cr/Al ratios in samples collected April 2016 are about half that of October 2014 samples, except for samples CR-6 and CR-8, which have higher Cr/Al in April than October (Table 3). These observations are consistent with presumably higher sediment load in the Spring, and a lower reactive/detrital Cr ratio in the suspended material, as discussed above.

For October 2014 water samples, there is a general shift to more positive δ^{53}Cr values moving downstream, with one exception (CR-3) (Fig. 5A). However, this same trend was not observed in April 2016 samples. The systematic downstream increase in δ^{53}Cr in October is unlikely cased by partial reduction during transport, as partial reduction would have caused dissolved Cr concentrations to decrease as Cr moves downstream, which is not clearly observed (Fig. 5B). Interestingly, the δ^{53}Cr values of suspended particles and river bottom sediments also increases upstream to downstream (Fig. 5C and E, respectively). This suggests that source rocks may have controlled the δ^{53}Cr values of suspended sediment, bottom sediment, and river water samples.

6.6. Implications for river Cr flux to the ocean

According to our measured Cr concentrations (0.12 ± 0.06 ng/mL for total dissolved and 0.92 ± 0.35 ng/mL for suspended Cr) and previously published water flux data (560 m^3/s, Connecticut River Watershed Council; Gordon, 1980), the dissolved and suspended Cr fluxes of the Connecticut River into the Long Island Sound are 2.12 tons/year (or 4.08×10^4 mol/year) and 16.25 tons/year (or 3.13×10^5 mol/year), respectively. Therefore, Cr transport in the Connecticut River is dominated by the suspended load, consistent with previous findings (Kotaś and Stasicka, 2000 and references therein). The total dissolved Cr flux of the Connecticut River is about one to two orders lower than those of other rivers with similar discharges (see compilation in McClain and Maher, 2016). Such low dissolved Cr flux in the Connecticut River may be related to relatively low Cr concentration in the basement basalt (65 ± 25 μg/g, 2SD, based on the basalt samples in Table 2) compared to average upper crust (92 μg/g) and lower crust (215 μg/g) (Rudnick and Gao, 2003). It may also be related to very weak Cr leaching during weathering in the catchment, consistent with a limited decrease in Cr/Al ratios in bottom sediments and all catchment rocks (Fig. 6).

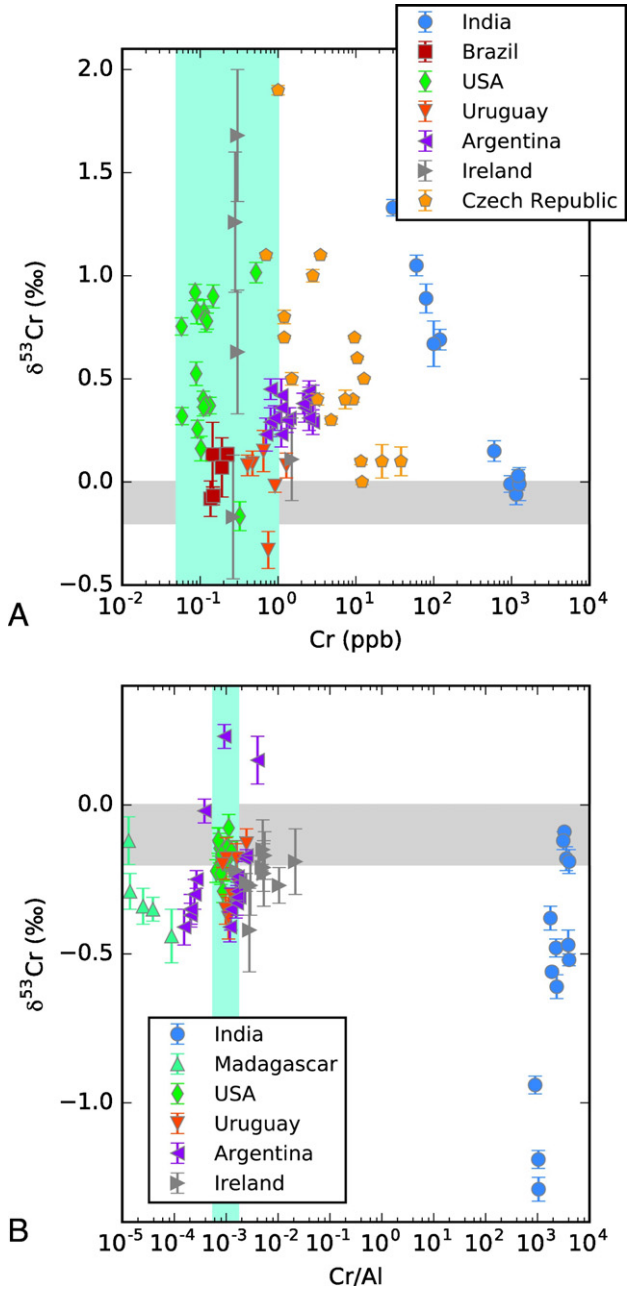

Fig. 7. Cr concentration and δ^{53}Cr of dissolved Cr in river water (A) and in residual weathered rocks (B) in previously published papers and in this study. Tropical climate: India and Madagascar. Temperate climate: USA, Uruguay, Argentina, and Ireland. The shaded blue vertical bar in A represents the average Cr concentration in rivers (Reinhard et al., 2013; McClain and Maher, 2016) (A) and Cr/Al (B) of the average continental crust. The gray horizontal bars represent the δ^{53}Cr ranges for the upper continental crust. Data sources: this study; Berger and Frei, 2014; Frei et al., 2014; Novak et al., 2014; Paulukat et al., 2015; D'Arcy et al., 2016. Some stream waters with total Cr concentrations higher than 1 ppm (because of anthropogenic or geogenic contamination; Farkaš et al., 2013; Novak et al., 2014) are excluded.

Previous δ^{53}Cr data of river input, ocean reservoir, and sediment sinks suggest a general mass imbalance. Global seawater has dissolved δ^{53}Cr values between 0.4‰ to 1.5‰ (e.g. Bonnand et al., 2013; Scheiderich et al., 2015), which is similar to rivers––the major contributor of Cr to the ocean (e.g., Frei et al., 2014; Novak et al., 2014; Paulukat et al., 2015; D'Arcy et al., 2016; this study). Another, but

smaller Cr input to the ocean is groundwater, which typically has higher δ^{53}Cr values compared to river water (e.g. Berna et al., 2010; Izbicki et al., 2012). Since reductive sequestration of dissolved Cr from the ocean is expected to push seawater to higher δ^{53}Cr values, it is expected that seawater δ^{53}Cr should be higher than river input. This discrepancy may be explained by lowering the average δ^{53}Cr value of the continental flux through release of isotopically light Cr from the suspended and/or organically complexed Cr load. In our Connecticut River water samples, only one (CR-1) has unfractionated δ^{53}Cr and high dissolved Cr, suggesting this water sample is dominated by dissolved, organic-complexed Cr(III). In contrast, all suspended samples have higher Cr concentrations and relatively unfractionated δ^{53}Cr compared to dissolved Cr samples. Thus, spatial heterogeneities in terms of parent rock lithology and dissolved organic content may explain the observed variable Cr values within a single river (e.g. this study), as well as global rivers (Frei et al., 2014; Novak et al., 2014; Paulukat et al., 2015; D'Arcy et al., 2016), and global seawater (Bonnand et al., 2013; Scheiderich et al., 2015). To our knowledge, this is the first report of δ^{53}Cr values for riverine suspended matter. Our data from the Connecticut River show that the suspended Cr flux is about an order of magnitude higher than the dissolved flux, suggesting suspended matter could potentially influence seawater Cr isotope values significantly. Therefore, future Cr isotope studies of river waters should consider both dissolved and suspended Cr.

6.7. Cr and its isotope fractionation in weathering profiles

Weathering of igneous rocks are expected to preferentially leach light Cr isotopes, leaving the residual weathered rock with relatively low Cr/Al ratio and negatively fractionated δ^{53}Cr (Crowe et al., 2013; Frei and Polat, 2013; Berger and Frei, 2014; Frei et al., 2014), although in black shale weathering environments δ^{53}Cr fractionation is absent or in the opposite direction (Wang et al., 2016b). In contrast to previous studies, weathering effects on Cr content and isotopic fractionation are small in the Connecticut River system (a basalt-dominated catchment). The Cr/Al ratios are similar to or slightly lower than the UCC (Rudnick and Gao, 2003), suggesting weak mobilization of Cr during weathering. The weathering profile samples (basalts, siltstones, and glacial tills) have δ^{53}Cr values similar to or smaller than the BSE (Fig. 6). The δ^{53}Cr values are at the lower end of, or slightly lower than the BSE in the residual catchment rocks and soils. They complement the positive δ^{53}Cr values in dissolved and suspended Cr. However, such subtle negative values suggest that only small portion of Cr is mobilized during weathering. Using the mean value of weathered rocks/soils and bottom sediments (−0.15‰), the mean bulk silicate earth value (−0.1‰) as the starting δ^{53}Cr before weathering, and individual dissolved Cr δ^{53}Cr values, a simple mass balance calculation shows that from 5% to 12% of Cr is weathered away from the source rocks into the Connecticut River.

It would be useful to compare these values with values from a tropical climate. Two other studies have reported Cr isotope systematics in tropical climates––India (Paulukat et al., 2015) and Madagascar (Berger and Frei, 2014). The δ^{53}Cr values of weathered rock from India range from −1.29‰ to −0.12‰, and δ^{53}Cr values of weathered rock from Madagascar range from −0.57‰ to −0.12‰, lower than those in the Connecticut River system and BSE (Fig. 7B and Fig. 8B). In contrast, the δ^{53}Cr of dissolved Cr between the two climate systems show very small (but significant, $p < 0.001$) differences (Fig. 7A and Fig. 8A). Such small difference, with a bootstrapped mean of 0.47‰ for the Connecticut River and 0.53‰ for the Damsal River, is within current analytical error (±0.07–0.09‰).

It is important to note the lithologic differences between the Connecticut River in USA (basalt) and the Damsal River in India (chromite). Lithology is thought to be a dominant factor controlling weathering rates in watersheds, with mineral weatherability decreasing in the order from carbonate > mafic silicates > feldspars > quartz (White and Blum, 1995 and refs therein). Such variable weatherability of catchment rocks may have significant effect on the overall Cr mobility (e.g. Oze et al., 2004a, 2004b) and isotope fractionation, as reaction timescales can influence kinetic isotope fractionation (e.g. Sikora et al., 2008; Basu and Johnson, 2012; Basu et al., 2014; Jamieson-Hanes et al., 2012) and isotope exchange between reduced and oxidized Cr(VI) (e.g. Wang et al., 2015). The Madagascar study investigated a laterite profile developed on a granitoid bedrock, but no dissolved Cr data were reported. In order to have more rigorous comparison between different climate systems, more Cr studies of different catchment rocks in tropical areas are needed.

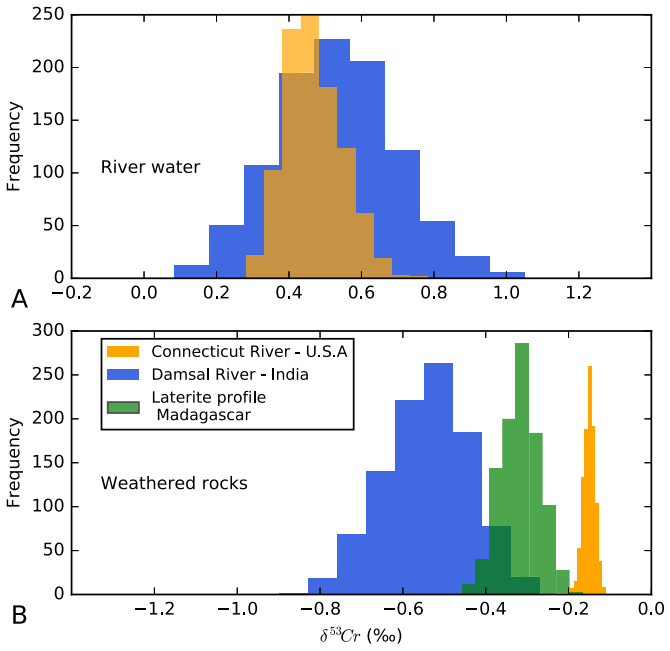

Fig. 8. Histograms of the bootstrapped (1000 times) mean δ^{53}Cr in temperate (the Connecticut River in U.S.A.) and tropical (the Damsal River in India) climates: dissolved Cr in A and weathered rocks in B. P value for the comparison between dissolved δ^{53}Cr in the Connecticut River (CR) and Damsal River (DR) is <0.001, but the difference in the bootstrapped means (mean CR = 0.47‰, mean DR = 0.53‰) is within the current analytical error (±0.07–0.09‰).

6.8. Climate effects on Cr isotope systematics in weathering environments

Apart from lithology effects on Cr isotopic systematics during weathering, climate may also play a role. Many studies have shown a dependence of weathering rates on climate (temperature, rainfall, and runoff) (e.g., Meybeck, 1987; White and Blum, 1995; Gaillardet et al., 1999; Millot et al., 2002; Oliva et al., 2003; Wu et al., 2013; Li et al., 2016). Therefore, precipitation and temperature effects should be considered when modeling the feedback between climate and chemical weathering rates, especially the influence of tropical regions on global silicate weathering fluxes (White and Blum, 1995). Runoff and temperature also positively influence weathering rates (e.g., Millot et al., 2002). Hydrochemical data of 99 small watersheds in granitic environments show that the highest weathering rate was obtained for tropical zone warm watersheds (Oliva et al., 2003). Therefore, it is expected that the weathering of different climate regions as well as lithological differences will have important effects on the release, migration, and fractionation of Cr.

Tropical soils are typically wetter and contain more organic matter with shorter residence times compared to temperate soils (Trumbore, 1993). Dissolved organic matter can promote Cr(VI) reduction (e.g. Wittbrodt and Palmer, 1997; Gu and Chen, 2003), and thus may inhibit Cr(III) oxidation during weathering because of the relative chemical inertness of Cr(III)-ligand complexes (Cotton et al., 1980). It has been

proposed that organic rich weathering environments (e.g. top soils) may be a sink of Cr rather than a source of Cr to runoff (e.g. Frei et al., 2014; Wang et al., 2016b). However, soil and dissolved organic matter were not analyzed in our study or studies of other weathering environments, and therefore we do not yet understand the relationship between dissolved organic matter, dissolved Cr content and δ^{53}Cr in weathering environments.

For assessing the influence of climate and lithology on Cr isotope fractionation, we compare our data with previous studies focused on tropical and temperate weathering environments (Crowe et al., 2013; Berger and Frei, 2014; Paulukat et al., 2015; D'Arcy et al., 2016) (Fig. 7A). The dissolved Cr concentrations in the Connecticut River are at the low end of published river water data. There is no systematic trend in Cr concentration and δ^{53}Cr between temperate (USA, Argentina, Uruguay, Ireland, and Czech Republic) and tropical (India and Brazil) zones, suggesting that climate is not a major control of riverine Cr concentrations. Other factors––such as weatherability of parent rocks and dissolved organic contents as discussed above––may play important roles. For example, in catchments with ultramafic rocks, river Cr(VI) concentrations reach as high as >20 μg/mL (Farkaš et al., 2013; Novak et al., 2014; Paulukat et al., 2015).

Like river waters, the Cr/Al and δ^{53}Cr values in weathered rocks do not show systematic correlation with climate zones (Fig. 7B). For example, two tropical climate weathering profiles in India and Madagascar have very different Cr/Al and δ^{53}Cr values. The very negative laterite δ^{53}Cr values in India (as low as −1.29‰) were attributed to the extreme intensive weathering of heterogeneously layered ultramafic Cr-rich rocks (Paulukat et al., 2015). However, the laterite samples in Madagascar have δ^{53}Cr values distinguishable from those in temperate climate zones. These observations suggest that Cr isotope fractionation during weathering is not a simple function of general climate type, but could be controlled by parent rock lithology and denudation rates. As observed previously, different Cr(III)-minerals have different weatherability (e.g. spinels are more resistant than igneous and metamorphic silicates, Oze et al., 2004a, 2004b), which, combined with the availability of manganese oxides, control the mobilization of Cr(III) to Cr(VI) and accompanied isotope fractionation (e.g. Eary and Rai, 1987; Bain and Bullen, 2005; Oze et al., 2007). The denudation timescales of soil profiles affect the timescales of contact between Cr(III) and manganese oxides - which controls the oxidation of Cr(III), and between Cr(VI) and Cr(III) - which might shift δ^{53}Cr values due to isotope exchange between the two valence states (Altman and King, 1961; Schauble et al., 2004; Wang et al., 2015).

The lack of clear climate signal on surface Cr isotope systematics suggests that the isotopic composition of the Cr terrestrial flux to the ocean does not vary dramatically on short times scales associated with climate shifts, and thus Cr isotopes may be a robust paleoceanographic tracers (e.g., Holmden et al., 2016; Wang et al., 2016c).

7. Conclusions

The δ^{53}Cr values of the dissolved Cr in the Connecticut River water is elevated from the weathering profiles by up to ~1‰. Seasonal effect on dissolved Cr concentration and δ^{53}Cr was observed in some but not all tributaries. In contrast, δ^{53}Cr values of suspended matters show a small but systematic seasonal difference: within the BSE in April but ~0.1‰ higher than the BSE in October. This seasonal effect on suspended Cr concentration and δ^{53}Cr is attributed to increased silicate and oxide load in spring seasons with stronger hydrological fluxes. The positively fractionated dissolved and suspended Cr is complemented by residual weathered rocks represented by several weathering profiles and river bottom sediments, which have δ^{53}Cr values at the lower end of, or slightly more negative than the unfractionated BSE.

Although suspended δ^{53}Cr is only slightly fractionated from BSE, its annual flux is about 10 times higher than dissolved Cr load in the Connecticut River. If this relationship holds in other globally distributed rivers, the suspended Cr load can potentially influence the isotopic composition of dissolved Cr in the coastal and open ocean water. Therefore, the concentration and isotopic composition of suspended Cr should be studied in more detail in future studies.

A compilation of the Cr isotopic compositions and concentrations in river waters and weathered rocks from different climate zones suggest that Cr isotope fractionation during weathering is not a simple function of climate but is influenced by multiple factors such as lithology of parent rocks and content of dissolved organic matter in weathering fluids.

Acknowledgements

This work was supported by the State Scholarship Fund (No. 201406195032) from the China Scholarship Council, the Natural Science Foundation of China (Project No. 41373003) to Weihua Wu, the Agouron Institute Postdoctoral Fellowship (AI-F-GB31.14.2) to Xiangli Wang, and the NASA Alternative Earth's NAI and Sloan Fellowships to Noah Planavsky and Christopher T. Reinhard. Thanks to Mark Brandon for collecting the Amazon River samples. Finally, we would like to thank three anonymous reviewers for their constructive comments that greatly improved the quality of the manuscript.

References

Altman, C., King, E.L., 1961. The mechanism of the exchange of chromium(III) and chromium(VI) in acidic solutions. J. Am. Chem. Soc. 83, 2825–2830.
Babechuk, M.G., Kleinhanns, I.C., Schoenberg, R., 2016. Chromium geochemistry of the ca. 1.85 Ga Flin Flon paleosol. Geobiology 1–21.
Bain, D.J., Bullen, T.D., 2005. Chromium isotope fractionation during oxidation of Cr (III) by manganese oxides. Geochim. Cosmochim. Acta 69, S212.
Ball, J.W., Izbicki, J., 2004. Occurrence of hexavalent chromium in ground water in the western Mojave Desert, California. Appl. Geochem. 19, 1123–1135.
Bartlett, R.J., James, B., 1979. Behavior of chromium in soils: III. Oxidation. J. Environ. Qual. 8, 31–35.
Bartlett, R.J., James, B.R., 1988. Mobility and bioavailability of chromium in soils. In: Nriagu, J.O., Nierboor, E. (Eds.), Chromium in the Natural and Human Environments. John Wiley and Sons, New York, pp. 267–383.
Bartlett, R.J., Kimble, J.M., 1976a. Behavior of chromium in soils: I. Trivalent forms. J. Environ. Qual. 5, 370–383.
Bartlett, R.J., Kimble, J.M., 1976b. Behavior of chromium in soils: II. Hexavalent forms. J. Environ. Qual. 5, 383–386.
Basu, A., Johnson, T.M., 2012. Determination of hexavalent chromium reduction using Cr stable isotopes: isotopic fractionation factors for permeable reactive barrier materials. Environ. Sci. Technol. 46, 5353–5360.
Basu, A., Johnson, T.M., Sanford, R.A., 2014. Cr isotope fractionation factors for Cr (VI) reduction by a metabolically diverse group of bacteria. Geochim. Cosmochim. Acta 142, 349–361.
Berger, A., Frei, R., 2014. The fate of chromium during tropical weathering: a laterite profile from Central Madagascar. Geoderma 213, 521–532.
Berna, E.C., Johnson, T.M., Makdisi, R.S., Basu, A., 2010. Cr stable isotopes as indicators of Cr (VI) reduction in groundwater: a detailed time-series study of a point-source plume. Environ. Sci. Technol. 44, 1043–1048.
Bodek, I., Lyman, W.J., Reehl, W.F., Rosenblatt, D.H., 1988. In: Bodek, I. (Ed.), Environmental Inorganic Chemistry Properties, Processes, and Estimation Methods. Pergamon Press, New York.
Bonnand, P., Parkinson, I.J., James, R.H., Karjalainen, A.-M., Fehr, M.A., 2011. Accurate and precise determination of stable Cr isotope compositions in carbonates by double spike MC-ICP-MS. J. Anal. At. Spectrom. 26, 528–535.
Bonnand, P., James, R., Parkinson, I., Connelly, D., Fairchild, I., 2013. The chromium isotopic composition of seawater and marine carbonates. Earth Planet. Sci. Lett. 382, 10–20.
Cole, D.B., Reinhard, C.T., Wang, X., Gueguen, B., Halverson, G.P., Gibson, T., Hodgskiss, M.S., McKenzie, N.R., Lyons, T.W., Planavsky, N.J., 2016. A shale-hosted Cr isotope record of low atmospheric oxygen during the Proterozoic. Geology G37787, 1.
Comber, S., Gardner, M., 2003. Chromium redox speciation in natural waters. J. Environ. Monit. 5, 410–413.
Cotton, F.A., Ilsley, W.H., Kaim, W., 1980. Sensitivity of the Cr—Cr quadruple bond to axial interactions in dichromium(II) compounds. J. Am. Chem. Soc. 102 (10).
Crowe, S.A., Døssing, L.N., Beukes, N.J., Bau, M., Kruger, S.J., Frei, R., Canfield, D.E., 2013. Atmospheric oxygenation three billion years ago. Nature 501, 535–538.
D'Arcy, J., Babechuk, M.G., Døssing, L.N., Gaucher, C., Frei, R., 2016. Processes controlling the chromium isotopic composition of river water: constrains from basaltic river catchments. Geochim. Cosmochim. Acta 186, 296–315.
Das, A., Krishnaswami, S., 2007. Elemental geochemistry of river sediments from the Deccan Traps, India: implications to sources of elements and their mobility during basalt–water interaction. Chem. Geol. 242, 232–254.
Dojlido, J.B., Best, G.A., 1993. Chemistry of Water and Water Pollution. Ellis Horwood Limited, Chichester, UK.

Døssing, L., Didderiksen, K., Stipp, S.L.S., Frei, R., 2011. Reduction of hexavalent chromium by ferrous iron: a process of chromium isotope fractionation and its relevance to natural environments. Chem. Geol. 285, 157–166.
Douglas, T.A., Chamberlain, C.P., Blum, J.D., 2002. Land use and geologic controls on the major elemental and isotopic (delta N-15 and Sr-87/Sr-86) geochemistry of the Connecticut River watershed, USA. Chem. Geol. 189, 19–34.
Du, X., Boonchayaanant, B., Wu, W.M., Fendorf, S., Bargar, J., Criddle, C.S., 2011. Reduction of uranium (VI) by soluble iron (II) conforms with thermodynamic predictions. Environ. Sci. Technol. 45, 4718–4725.
Eary, L.E., Rai, D., 1987. Kinetics of chromium (III) oxidation to chromium (VI) by reaction with manganese dioxide. Environ. Sci. Technol. 21, 1187–1193.
Eary, L.E., Rai, D., 1989. Kinetics of chromate reduction by ferrous ions derived from hematite and biotite at 25oC. Am. J. Sci. 289, 180–213.
Elderfield, H., 1970. Chromium speciation in sea water. Earth Planet. Sci. Lett. 9, 10–16.
Ellis, A.S., Johnson, T.M., Bullen, T.D., 2002. Chromium isotopes and the fate of hexavalent chromium in the environment. Science 295, 2060–2062.
Ellis, A.S., Johnson, T.M., Bullen, T.D., 2004. Using chromium stable isotope ratios to quantify Cr (VI) reduction: lack of sorption effects. Environ. Sci. Technol. 38, 3604–3607.
Ellis, A.S., Johnson, T.M., Villalobos-Aragon, A., Bullen, T., 2008. Environmental cycling of Cr using stable isotopes: kinetic and equilibirum effects. Abstract H53F-08 Presented at 2008 AGU Fall Meeting, San Francisco, CA.
Farkaš, J., Chrastny, V., Novak, M., Cadkova, E., Pasava, J., Chakrabarti, R., Jacobsen, S.B., Ackerman, L., Bullen, T.D., 2013. Chromium isotope variations ($\delta^{53/52}$Cr) in mantle-derived sources and their weathering products: Implications for environmental studies and the evolution of $\delta^{53/52}$Cr in the Earth's mantle over geologic time. Geochim. Cosmochim. Acta 123, 74–92.
Fendorf, S.E., 1995. Surface reactions of chromium in soils and waters. Geoderma 67, 55–71.
Fendorf, S.E., Li, G., 1996. Kinetics of chromate reduction by ferrous iron. Environ. Sci. Technol. 30, 1614–1617.
Fendorf, S.E., Zasoski, R.J., 1992. Chromium (III) oxidation by δ-MnO_2. Environ. Sci. Technol. 26, 79–85.
Freeze, R.A., Cherry, J.A., 1979. In: Brenn, C., McNeily, K. (Eds.), Groundwater. Prentice-Hall, Englewood Cliffs, New Jersey.
Frei, R., Polat, A., 2013. Chromium isotope fractionation during oxidative weathering-implications from the study of a Paleoproterozoic (ca. 1.9 Ga) paleosol, Schreiber Beach, Ontario, Canada. Precambrian Res. 224, 434–453.
Frei, R., Gaucher, C., Poulton, S.W., Canfield, D.E., 2009. Fluctuations in Precambrian atmospheric oxygenation recorded by chromium isotopes. Nature 461, 250–253.
Frei, R., Poiré, D., Frei, K.M., 2014. Weathering on land and transport of chromium to the ocean in a subtropical region (Misiones, NW Argentina): a chromium stable isotope perspective. Chem. Geol. 381, 110–124.
Gaillardet, J., Dupré, B., Louvat, P., Allègre, C.J., 1999. Global silicate weathering and CO_2 consumption rates deduced from the chemistry of large rivers. Chem. Geol. 159, 3–30.
Gilleaudeau, G., Frei, R., Kaufman, A., Kah, L., Azmy, K., Bartley, J., Chernyavskiy, P., Knoll, A., 2016. Oxygenation of the mid-Proterozoic atmosphere: clues from chromium isotopes in carbonates. Geochem. Perspect. Lett. 2, 178–187.
Gordon, R.B., 1980. The sedimentary system of Long Island Sound. Adv. Geophys. 22, 1–39.
Graham, A.M., Bouwer, E.J., 2009. Rates of hexavalent chromium reduction in anoxic estuarine sediments: pH effects and the role of acid volatile sulfides. Environ. Sci. Technol. 44, 136–142.
Grohse, P.M., Gutknecht, W.F., Hodson, L., Wilson, B.M., 1988. The Fate of Hexavalent Chromium in the Atmosphere, Research Triangle Institute Report on CARB Contract #A6-096-32, Report Number ARB/R-89/379. California Air Resources Board.
Gu, B., Chen, J., 2003. Enhanced microbial reduction of Cr(VI) and U(VI) by different natural organic matter fractions. Geochim. Cosmochim. Acta 67, 3575–3582.
Gueguen, E., Reinhard, C.T., Algeo, T.J., Peterson, L.C., Nielsen, S.G., Wang, X.L., Rowe, H., Planavsky, N.J., 2016. The chromium isotope composition of reducing and oxic marine sediments. Geochim. Cosmochim. Acta 184, 1–19.
Han, R., Qin, L., Brown, S.T., Christensen, J.N., Beller, H.R., 2012. Differential isotopic fractionation during Cr(VI) reduction by an aquifer-derived bacterium under aerobic versus denitrifying conditions. Appl. Environ. Microbiol. 78, 2462–2464.
Holmden, C., Jacobson, A., Sageman, B., Hurtgen, M., 2016. Response of the Cr isotope proxy to cretaceous ocean anoxic event 2 in a pelagic carbonate succession from the western interior seaway. Geochim. Cosmochim. Acta 186, 277–295.
Izbicki, J.A., Bullen, T.D., Martin, P., Schroth, B., 2012. Delta chromium-53/52 isotopic composition of native and contaminated groundwater, Mojave Desert, USA. Appl. Geochem. 27, 841–853.
James, B.R., Bartlett, R.J., 1983a. Behavior of chromium in soils: V. Fate of organically complexed Cr(III) added to soil. J. Environ. Qual. 12, 169–172.
James, B.R., Bartlett, R.J., 1983b. Behavior of chromium in soils: VI. Interactions between oxidation-reduction and organic complexation. J. Environ. Qual. 12, 173–176.
James, B.R., Bartlett, R.J., 1983c. Behavior of chromium in soils: VII. Adsorption and reduction of hexavalent forms. J. Environ. Qual. 12, 177–181.
Jamieson-Hanes, J.H., Gibson, B.D., Lindsay, M.B.J., Kim, Y., Ptacek, C.J., Blowes, D.W., 2012. Chromium isotope fractionation during reduction of Cr (VI) under saturated flow conditions. Environ. Sci. Technol. 46, 6783–6789.
Jeandel, C., Minster, J., 1987. Chromium behavior in the ocean: global versus regional processes. Glob. Biogeochem. Cycles 1, 131–154.
Johnson, T.M., Herbel, M.J., Bullen, T.D., Zawislanski, P.T., 1999. Selenium isotope ratios as indicators of selenium sources and oxyanion reduction. Geochim. Cosmochim. Acta 63, 2775–2783.
Kieber, R.J., Willey, J.D., Zvalaren, S.D., 2002. Chromium speciation in rainwater: temporal variability and atmospheric deposition. Environ. Sci. Technol. 36, 5321–5327.
Kim, C., Zhou, Q., Deng, B., Thornton, E.C., Xu, H., 2001. Chromium(VI) reduction by hydrogen sulfide in aqueous media: stoichiometry and kinetics. Environ. Sci. Technol. 35, 2219–2225.
Kimbrough, D.E., Cohen, Y., Winer, A.M., Creelman, L., Mabuni, C., 1999. A critical assessment of chromium in the environment. Crit. Rev. Environ. Sci. Technol. 29, 1–46.
Kitchen, J.W., Johnson, T.M., Bullen, T.D., Zhu, J., Raddatz, A., 2012. Chromium isotope fractionation factors for reduction of Cr(VI) by aqueous Fe(II) and organic molecules. Geochim. Cosmochim. Acta 89, 190–201.
Kotaš, J., Stasicka, Z., 2000. Chromium occurrence in the environment and methods of its speciation. Environ. Pollut. 263–283.
Li, G.J., Hartmann, J., Derry, L.A., West, A.J., You, C.-F., Long, X.Y., Zhan, T., Li, L.F., Li, G., Qiu, W.H., Li, T., Liu, L.W., Chen, Y., Ji, J.F., Zhao, L., Chen, J., 2016. Temperature dependence of basalt weathering. Earth Planet. Sci. Lett. 443, 59–69.
Manceau, A., Charlet, L., 1992. X-ray absorption spectroscopic study of the sorption of Cr(III) at the oxide-water interface: I. Molecular mechanism of Cr(III) oxidation on Mn oxides. J. Colloid Interface Sci. 148 (2), 425–442.
McClain, C.N., Maher, K., 2016. Chromium fluxes and speciation in ultramafic catchments and global rivers. Chem. Geol. 426, 135–157.
Meybeck, M., 1987. Global chemical weathering of surficial rocks estimated from river dissolved loads. Am. J. Sci. 287, 401–428.
Millot, R., Gaillardet, J., Dupré, B., Allègre, C.J., 2002. The global control of silicate weathering rates and the coupling with physical erosion: new insights from rivers of the Canadian Shield. Earth Planet. Sci. Lett. 196, 83–98.
Nakayama, E., Kuwamoto, T., Tsurubo, S., Fujinaga, T., 1981. Chemical speciation of chromium in sea water: Part 2. Effects of manganese oxides and reducible organic materials on the redox processes of chromium. Anal. Chim. Acta 130, 401–404.
Neubert, N., Heri, A.R., Voegelin, A.R., Nägler, T.F., Schlunegger, F., Villa, I.M., 2011. The molybdenum isotopic composition in river water: constraints from small catchments. Earth Planet. Sci. Lett. 304, 180–190.
Novak, M., Chrastny, V., Čadková, E., Farkas, J., Bullen, T., Tylcer, J., Szurmanova, Z., Cron, M., Prechova, E., Curik, J., 2014. Common occurrence of a positive δ^{53}Cr shift in Central European waters contaminated by geogenic/industrial chromium relative to source values. Environ. Sci. Technol. 48, 6089–6096.
Oliva, P., Viers, J., Dupré, B., 2003. Chemical weathering in granitic environments. Chem. Geol. 202, 225–256.
Oze, C., Fendorf, S.E., Bird, D.K., Coleman, R., 2004a. Chromium geochemistry in serpentinized ultramafic rocks and serpentine soils in the Franciscan Complex of California. J. Am. Sci. 304, 67–101.
Oze, C., Fendorf, S.E., Bird, D.K., Coleman, R., 2004b. Chromium geochemistry of serpentine soils. Int. Geol. Rev. 46, 97–126.
Oze, C., Bird, D.K., Fendorf, S., 2007. Genesis of hexavalent chromium from natural sources in soil and groundwater. Proc. Natl. Acad. Sci. U. S. A. 104, 6544–6549.
Oze, C., Sleep, N.H., Coleman, R.G., Fendorf, S., 2016. Anoxic oxidation of chromium. Geology G37844:37841. http://dx.doi.org/10.1130/G37844.1.
Patterson, R.R., Fendorf, S., Fendorf, M., 1997. Reduction of hexavalent chromium by amorphous iron sulfide. Environ. Sci. Technol. 31, 2039–2044.
Paulukat, C., Døssing, L.N., Mondal, S.K., Voegelin, A.R., Frei, R., 2015. Oxidative release of chromium from Archean ultramafic rocks, its transport and environmental impact – a Cr isotope perspective on the Sukinda valley ore district (Orissa, India). Appl. Geochem. 59, 125–138.
Pettine, M., D'Ottone, L., Campanella, L., Millero, F.J., Passino, R., 1998. The reduction of chromium (VI) by iron (II) in aqueous solutions. Geochim. Cosmochim. Acta 62, 1509–1519.
Planavsky, N.J., Reinhard, C.T., Wang, X., Thomson, D., McGoldrick, P., Rainbird, R.H., Johnson, T., Fischer, W.W., Lyons, T.W., 2014. Low Mid-Proterozoic atmospheric oxygen levels and the delayed rise of animals. Science 346, 635–638.
Raddatz, A.L., Johnson, T.M., McLing, T.L., 2011. Cr stable isotopes in Snake River plain aquifer groundwater: evidence for natural reduction of dissolved Cr(VI). Environ. Sci. Technol. 45, 502–507.
Rai, D., Sass, B.M., Moore, D.A., 1987. Chromium(III) hydrolysis constants and solubility of chromium(III) hydroxide. Inorg. Chem. 26, 345–349.
Rai, D., Eary, L.E., Zachara, J.M., 1989. Environmental chemistry of chromium. Sci. Total Environ. 86, 15–23.
Reed, J.C., Wheeler, J.O., Tucholke, B.E., compilers, 2004. Geologic Map of North America: Decade of North American Geology Continental Scale Map 001, Boulder, Geological Society of America, Scale 1:5,000,000.
Reinhard, C.T., Planavsky, N.J., Robbins, L.J., Partin, C.A., Gill, B.C., Lalonde, S.V., Bekker, A., Konhauser, K.O., Lyons, T.W., 2013. Proterozoic ocean redox and biogeochemical stasis. Proc. Natl. Acad. Sci. U. S. A. 110, 5357–5362.
Reinhard, C.T., Planavsky, N.J., Wang, X., Fischer, W.W., Johnson, T.M., Lyons, T.W., 2014. The isotopic composition of authigenic chromium in anoxic marine sediments: a case study from the Cariaco Basin. Earth Planet. Sci. Lett. 407, 9–18.
Ross, D.S., Sjogren, R.E., Bartlett, R.J., 1981. Behavior of chromium in soils: IV. Toxicity to microorganisms. J. Environ. Qual. 10, 145–148.
Rudnick, R.L., Gao, S., 2003. Composition of the continental crust. In: Turekian, K., Holland, H.D. (Eds.), Treatise on Geochemistry. Pergamon, Oxford, pp. 1–64.
Sass, B.M., Rai, D., 1987. Solubility of amorphous chromium (III)-iron(III) solid solution. Inorg. Chem. 26, 2228–2232.
Schauble, E., Rossman, G.R., Taylor Jr., H.P., 2004. Theoretical estimates of equilibrium chromium-isotope fractionations. Chem. Geol. 205, 99–114.
Scheiderich, K., Amini, M., Holmden, C., Francois, R., 2015. Global variability of chromium isotopes in seawater demonstrated by Pacific, Atlantic, and Arctic Ocean samples. Earth Planet. Sci. Lett. 423, 87–97.
Schoenberg, R., Zink, S., Staubwasser, M., von Blanckenburg, F., 2008. The stable Cr isotope inventory of solid Earth reservoirs determined by double spike MC-ICP-MS. Chem. Geol. 249, 294–306.

Schroeder, R.L., Lee, G.F., 1975. Potential transformation of chromium in natural waters. Water, Air, Soil Pollut. 4, 355–365.
Sikora, E.R., Johnson, T.M., Bullen, T.D., 2008. Microbial mass-dependent fractionation of chromium isotopes. Geochim. Cosmochim. Acta 72, 3631–3641.
Trumbore, S.E., 1993. Comparison of carbon dynamics in tropical and temperate soils using radiocarbon measurements. Glob. Biogeochem. Cycles 7, 275–290.
Vanderveen, C., Huizenga, J., 1981. Combatting river pollution taking the Rhine as an example. Water Sci. Technol. 13, 1035–1059.
Wang, D.T., Fregoso, D.C., Ellis, A.S., Johnson, T.M., Bullen, T.D., 2010. Stable Isotope Fractionation During Chromium(III) Oxidation by δ-MnO_2. Abstract H53F-1109 Presented at 2010 Fall Meeting. AGU, San Francisco, CA.
Wang, X.L., Johnson, T.M., Ellis, A.S., 2015. Equilibrium Isotopic Fractionation and Isotopic Exchange Kinetics between Cr (III) and Cr (VI). Geochim. Cosmochim. Acta 153, 72–90.
Wang, X.L., Planavsky, N., Hull, P., Tripati, A., Reinhard, C., Zou, H., Elder, L., Henehan, M., 2016a. Chromium isotopic composition of core-top planktonic foraminifera. Geobiology 1–14.
Wang, X.L., Planavsky, N.J., Reinhard, C.T., Zou, H., Ague, J.J., Wu, Y., Gill, B.C., Schwarzenbach, E.M., Peucker-Ehrenbrink, B., 2016b. Chromium isotope fractionation during subduction-related metamorphism, black shale weathering, and hydrothermal alteration. Chem. Geol. 429, 19–33.
Wang, X.L., Reinhard, C., Planavsky, N., Owens, J.D., Lyons, T., Johnson, C.M., 2016c. Sedimentary chromium isotopic compositions across the cretaceous OAE2 at demerara rise site 1258. Chem. Geol. 429, 85–92.
Wanner, C., Zink, S., Eggenberger, U., Mader, U., 2012. Assessing the Cr(VI) reduction efficiency of a permeable reactive barrier using Cr isotope measurements and 2D reactive transport modeling. J. Contam. Hydrol. 131, 54–63.
White, A.F., Blum, A.E., 1995. Effects of climate on chemical weathering in watersheds. Geochim. Cosmochim. Acta 59, 1729–1747.
Wielinga, B., Mizuba, M.M., Hansel, C.M., Fendorf, S., 2001. Iron promoted reduction of chromate by dissimilatory iron-reducing bacteria. Environ. Sci. Technol. 35, 522–527.
Wilber, W.G., Hunter, J.V., 1977. Aquatic Transport of Heavy-Metals in Urban-Environment. Water Resour. Bull. 13, 721–734.
Wittbrodt, P.R., Palmer, C.D., 1997. Reduction of Cr(VI) by soil humic acids. Eur. J. Soil Sci. 48, 151–162.
Wu, W.H., Zheng, H.B., Yang, J.D., Luo, C., Zhou, B., 2013. Chemical weathering, atmospheric CO_2 consumption, and the controlling factors in a subtropical metamorphic-hosted watershed. Chem. Geol. 356, 141–150.
Xu, F., Ma, T., Zhou, L., Hu, Z., Shi, L., 2015. Chromium isotopic fractionation during Cr(VI) reduction by *Bacillus* sp. under aerobic conditions. Chemosphere 130, 46–51.
Zink, S., Schoenberg, R., Staubwasser, M., 2010. Isotopic fractionation and reaction kinetics between Cr(III) and Cr(VI) in aqueous media. Geochim. Cosmochim. Acta 74, 5729–5745.